Carbohydrate Polymers 85 (2011) 560–564

Contents lists available at ScienceDirect

Carbohydrate Polymers

journal homepage: www.elsevier.com/locate/carbpol

Chemical compositions, infrared spectroscopy, and X-ray diffractometry study on brown-rotted woods

Gai-Yun Li [a], Luo-Hua Huang [a], Chung-Yun Hse [b], Te-Fu Qin [a,*]

[a] Research Institute of Wood Industry, Chinese Academy of Forestry, Xiangshan Road, Haidian District, Beijing 100091, China
[b] Southern Research Station, USDA Forest Service, 2500 Shreveport Highway, Pineville, LA, USA, 71360

ARTICLE INFO

Article history:
Received 9 July 2010
Received in revised form 22 February 2011
Accepted 9 March 2011
Available online 16 March 2011

Keywords:
Brown-rot decay
Chemical component
Alkali solubility
Crystallinity
FTIR

ABSTRACT

The effect of brown-rot decay on the chemical composition and crystallinity of Masson pine was studied by exposing it to *Wolfiporia cocos* (Schwein.) Ryvarden and Gilbn. for durations of up to 15 weeks in the field. The holocellulose content, α-cellulose content, and wood crystallinity decreased slowly in the initial stage, followed by a significant reduction during the late stage. Pentosans did not have a significant reduction until 15-week decay, indicating that pentosans were degraded much more slowly than the cellulose. Strong correlations between the holocellulose and lignin content and alkali solubility, wood crystallinity, and IR band height ratio indicated that different wood properties affected each other during the degradation process. The results indicated that the slight degradation of amorphous cellulose and hemicellulose formed the entrance points for *W. cocos* to attack crystalline cellulose, and led to the serious degradation of the cell wall.

1. Introduction

Brown-rot decay is one of the most destructive types of decay of wood in use. Brown-rot fungi mainly utilize the hemicellulose and cellulose of the cell wall (Green & Highley, 1997). Hemicellulose and cellulose are extensively degraded, while lignin is modified or slightly depolymerized (Jin, Schultz, & Nicholas, 1990). *Wolfiporia cocos* (Schwein.) Ryvarden and Gilbn., one species of brown-rot fungi, usually forms sclerotia on the roots of pine. The sclerotia of *W. cocos* is one of the most important crude drugs and has been used in Chinese traditional medicine for many centuries. It is also used in many Japanese Kampo formulae (Kubo et al., 2006). *W. cocos* is often cultivated in rural locations in China, Japan, and Korea. In addition, *W. cocos* was also found on palms and caused about 32% of weight loss after 12 weeks of incubation (Adaskaveg, Blanchette, & Gilbertson, 1991). Although the behaviors and mechanism of numerous wood decay fungi have been studied (Filley et al., 2002; Irbe et al., 2006; Winandy & Morrell, 1993), the majority of studies have been carried out in the laboratory. There have been no studies as to the chemical modifications and structural changes of wood decayed by *W. cocos* in the field.

The chemical composition changes in the wood measured by wet chemical analysis have been often investigated to understand the behaviors and mechanism of brown-rot decay. Crystallinity is an important property of wood, having effect on the physical, mechanical, and chemical properties of cellulose fibers (Lee, 1961). X-ray diffraction (XRD) has been for decades a rapid, non-destructive method to study wood crystallinity due to the diffraction peaks from cellulose crystals (Andersson, Serimaa, Paakkari, Saranpää, & Pesonen, 2003; Thygesen, Oddershede, Lilholt1, Thomsen, & Ståhl, 2005). More recently, Howell, Hastrup, Goodell, and Jellison (2009) thoroughly examined the changes in wood crystallinity caused by three different species of brown-rot fungi for 12 weeks. Fourier transform infrared (FTIR) has been used as a simple technique for analyzing the chemical and structural changes taking place in wood components due to chemical or physical treatments (Colom, Carrillo, Nogués, & Garriga, 2003; Pandey & Pitman, 2003; Popescu, Popescu, & Vasile, 2010). Compared to traditional methods, this technique needs minimal sample preparation and short analysis time.

The purpose of this study was to thoroughly characterize the change in wood chemical composition and crystallinity caused by *W. cocos* in the field test. The correlation between chemical composition, IR spectra, and crystallinity were also investigated in order to provide a new study method and information on the process of decay.

2. Methods

2.1. Materials

The brown-rot fungus used in this work was *Wolfiporia cocos* (Schwein.) Ryvarden and Gilbn. According to the outdoor cultivation method of *W. cocos* sclerotium (Wang, Wang, & Wang,

* Corresponding author. Tel.: +86 10 62889467; fax: +86 10 62889467.
E-mail addresses: tefuqin@yahoo.cn, qintefu@caf.ac.cn (T.-F. Qin).

0144-8617/$ – see front matter © 2011 Elsevier Ltd. All rights reserved.
doi:10.1016/j.carbpol.2011.03.014

2006), Masson pine (*Pinus massoniana* Lamb.) logs (approximately 70–80 cm-long × 9–15 cm in diameter) were buried in field soil and were incubated with the fungus. This experiment was carried out in Huangmei Hill, Yuexi County, Anhui Province, China, which is one of the cultivation sites of *W. cocos*. Incubation periods for the brown-rot fungi were 3, 7, 11, and 15 weeks. At each sampling time, 3–5 logs were removed, cleaned of any adhering soil and mycelium and air-dried. Wafers were cut from within the decay zone, combined from each replica and ground to pass through a 0.4 mm screen. Sound Masson pine wood powder was used as a control sample.

2.2. Chemical analysis

The klason lignin, holocellulose, α-cellulose, pentosan, and 1% sodium hydroxide solubility of the decayed woods were determined in accordance with the TAPPI standard T 222 om-98, T 249-75, T 203 om-93, T 223 cm-84, and T 212 om-98, respectively. All samples were analyzed in duplicate.

2.3. X-ray diffraction analysis

The relative crystallinity of wood was analyzed by a Philips X'Pert Pro X-ray diffractometer. The X-ray diffractograms were recorded from 0° to 40° at a scanning speed of 0.071°/s. The crystallinity index (CrI) was calculated using the Segal method (Segal, Creely, Martin, & Conrad, 1959) according to the following equation:

$$\mathrm{CrI}\,(\%) = \frac{I_{002} - I_{\mathrm{am}}}{I_{002}} \times 100$$

where I_{002} is the intensity of the diffraction from the (0 0 2) plane at $2\theta = 22.6^\circ$, representing both crystalline and amorphous material, and I_{am} is the intensity of the background scatter measured at $2\theta = 18.5^\circ$, representing only amorphous material.

2.4. FTIR spectroscopy analysis

FTIR spectra were obtained by direct transmittance using the KBr pellet technique. The spectra were recorded using a Perkin-Elmer Spectrum GX with a resolution of 4 cm^{-1} and 32 scans. Background spectra were obtained using a pure KBr pellet without any decayed wood sample. Peak height was measured with spectrum v3.02 software (Perkin-Elmer). The baseline was constructed by the connection of the lowest data points on either side of the peak. A vertical line was drawn from the top of the peak to the *X*-axis and the distance between the top of the peak and the baseline gave the peak height.

3. Results and discussion

3.1. Change of chemical composition due to decay

The main chemical compositions of the woods with different decay levels are presented in Table 1. It is regrettable that the weight mass of wood samples was not obtained due to the difficulties of field experiments. As shown in Table 1, the holocellulose contents had a gradual decrease before 7 weeks of decay, suggesting that the carbohydrate portions were already degraded by the attack of *W. cocos*. Thereafter a significant decrease in the holocellulose content was observed, indicating that the carbohydrate portions were suffering from strong degradation.

Although a changing trend of holocellulose with increasing decay was obtained, no clear tendency was observed related to cellulose and hemicellulose. Therefore, α-cellulose and pentosan were investigated to clarify the change trend of cellulose and hemicellulose, respectively. α-Cellulose generally stands for the undegraded, higher-molecular-weight cellulose. Compared to the α-cellulose content in sound wood of 46.91%, the value determined for decayed wood at week 3 was 40.49%, indicating that cellulose was already depolymerized in the initial 3 weeks. But the extensive and intensive depolymerization did not take place until 7-week decay, as shown in Table 1. In contrast, the pentosan content had only a very small change before 11 weeks of decay, followed by a rapid reduction from 13.20% at week 11 to 8.58% at week 15, indicating that pentosans were significantly attacked by *W. cocos* at 15-week decay. The above results indicate that the cellulose is degraded much faster than pentosans during the decay process of *W. cocos*.

Klason lignin (acid-insoluble) gradually increased before 7 weeks of decay. Then a continued remarkable increase was observed up to 15 weeks of decay. The change trend of Klason lignin was opposite to that of holocellulose during the brown-rotting process. The result was expected because the brown-rot fungi primarily utilize the carbohydrate portions of wood, and therefore, through residual enrichment, the (relative) lignin content increased with the degree of *W. cocos* attack. This conclusion was supported by the change trend of lignin to holocellulose ratio as shown in Table 1.

Alkali-soluble lignin content was also measured to provide further evidence for the change of lignin during degradation. The alkali-soluble lignin content almost did not change during the first 3 weeks incubation, but it rapidly increased from 2.37% at week 3 to 4.71% at week 7, followed by a notable increase up to 15 weeks, showing a similar change trend to that of Klason lignin. These phenomena can be also attributed to the significant degradation of carbohydrate portions of wood by *W. cocos*.

It was noticed that the sum of Klason lignin and holocellulose was 100% for sound sample, whereas the totals of decayed wood was lower than 100%. The reason for this phenomenon is possible that the holocellulose and Klason lignin fractions in decayed wood are not identical to the original components in sound wood due to chemical degradation. As a result, the degraded wood perhaps takes place with some different reactions from those of sound wood during analysis, which makes a part of the wood components analyzed as neither holocellulose nor lignin (Okino et al., 2008).

3.2. Change of 1% sodium hydroxide solubility due to decay

The solubility in 1% NaOH for samples exposed to *W. cocos* for different periods is given in Fig. 1. The alkali solubility increased from 12.89% to 17.90% after 3 weeks of decay. Thereafter, the alkali extractable contents showed a dramatic increase from 17.90% at week 3 to 70.07% at week 15. It was noticed that the change

Table 1
Chemical composition of Masson pine samples exposed to *W. cocos* for different durations.

Incubation time (weeks)	Holocellulose (%)	α-Cellulose (%)	Pentosan (%)	Klason lignin (%)	Alkali soluble lignin (%)	Ratio of lignin to holocellulose	Sum of lignin and holocellulose (%)
0	72.80	46.91	14.95	27.30	2.32	0.38	100.10
3	67.51	40.49	12.54	28.47	2.37	0.42	95.98
7	58.42	26.35	14.52	30.52	4.71	0.52	88.94
11	39.90	13.30	13.20	37.96	9.87	0.95	77.86
15	18.57	3.08	8.58	53.88	17.96	2.90	72.45

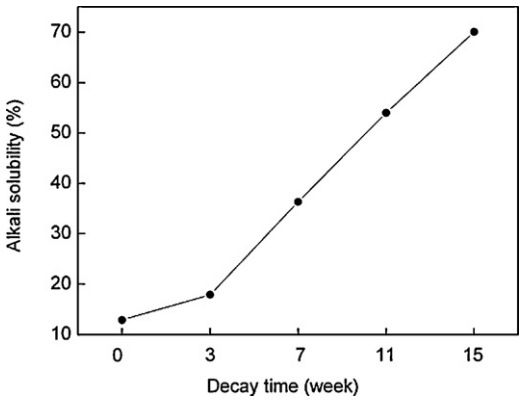

Fig. 1. Effect of decay time on 1% NaOH solubility.

trend of 1% NaOH solubility was similar to those of α-cellulose and alkali-soluble lignin content, all having a significant change at week 7, meaning that the evolution of 1% NaOH solubility was related closely to all the substantial changes in chemical compositions occurring during wood degradation process. Pettersen (1984) reported that wood solubility in 1% NaOH contained mostly extraneous components such as lignin, tannins, lipids, low molecular weight hemicelluloses and degraded cellulose. Therefore, the increment on the alkali extractive contents is attributed to the rapid depolymerization of cellulose by brown-rot fungi, as indicated by the rapid reduction of α-cellulose, and consequently small soluble low molecular weight fragments are produced and accumulated.

The quantitative correlations between the carbohydrate content, lignin content, and 1% NaOH solubility were studied. As expected, there was a good linear correlation ($R^2 = 0.86$) between the Klason lignin content and 1% NaOH solubility, and a very good linear correlation ($R^2 = 0.97$) between the holocellulose content and 1% NaOH solubility, which means that 1% NaOH solubility is more closely correlated with holocellulose than with lignin.

3.3. Relative crystallinity analysis

For a better understanding of the *W. cocos* degradation process, the relative crystallinity of wood was determined by XRD. Fig. 2 shows the X-ray diffractograms of sound and decayed wood. The

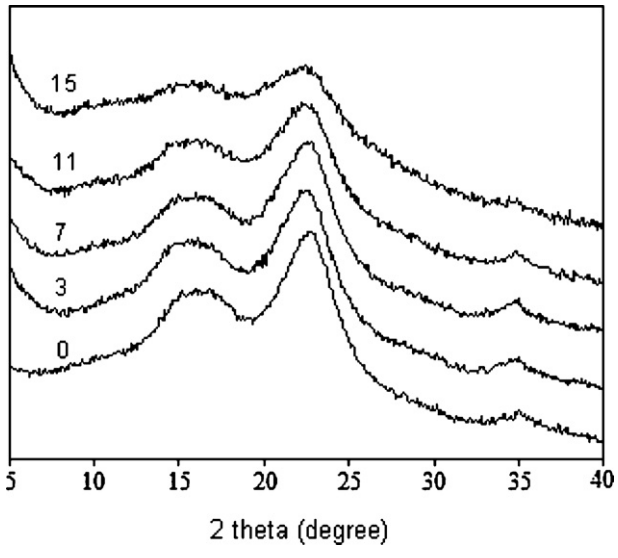

Fig. 2. X-ray diffractograms of Masson pine samples exposed to *W. cocos* for 0, 3, 7, 11 and 15 weeks.

Table 2
CrI of Masson pine samples exposed to *W. cocos* for different durations.

Incubation time (week)	0	3	7	11	15
C_rI (%)	40.3	39.0	37.6	28.9	16.1

sound wood displayed a typical X-ray diffractogram, having the major crystal planes of (1 0 1), (1 0 $\bar{1}$), (0 0 2) and (0 4 0) at around 14.5°, 16.5°, 22.6°, and 34.6°, respectively (Freire, Silvestre, Neto, Belgacem, & Gandini, 2006).

As shown in Fig. 2 and Table 2, the peak heights of four crystal planes had a slow decrease during the first 7 weeks, with CrI for the sound wood varying from 40.3% to 37.6%, indicating that the crystalline cellulose also became degraded at week 3. A drastic decrease in the peak heights of four crystal planes up to 15 weeks was observed after week 7, accompanied by a notable continuous decrease in CrI, changing from 37.6% at week 7 to 16.1% at week 15. This suggested that crystalline cellulose was suffering from continuing strong fungal attack. Amorphous cellulose is more readily available to fungi compared to crystalline cellulose, and the entrance points for *W. cocos* to attack crystalline cellulose normally need to be made by the first attack of amorphous cellulose (Moigne, Jardeby, & Navard, 2010). Considering the results of chemical compositions and CrI, it is speculated that cell wall components, especially the amorphous cellulose, are firstly attacked by *W. cocos*. As a result, pores and voids are formed in the cell wall. Then *W. cocos* move inside the cell wall through available pores and voids, and consequently both the outside and the inside of cell wall begin to be intensively attacked, leading to the serious degradation of the cell wall.

It was also noted that pentosans had a significant reduction at week 15, whereas CrI had a drastic decrease at week 11, indicating that serious degradation and removal of crystalline cellulose took place earlier than that of hemicellulose. It is known that hemicelluloses form an encrusting envelope around the cellulose microfibrils; further degradation and removal of cellulose may depend on previous degradation of the hemicellulose (Green & Highley, 1997). Thus, it is concluded that some entrances can be formed in the hemicellulose envelope in spite of the only slight degradation. It is not until the late stage of cellulose degradation that the extensive degradation of hemicellulose simultaneously happens.

Wellwood, Sastry, Micko, and Paszner (1974) reported that crystallinity significantly correlated (5% level) with the α-cellulose per tracheid but not with holocellulose. This prompts us to find the relationship between wood chemical compositions and cellulose crystallinity during decay. As expected, CrI was linearly related to the amount of main chemical components, giving a good correlation of $R^2 = 0.84$, 0.97, and 0.99 for α-cellulose, holocellulose and Klason lignin content, respectively. This result indicates that CrI depends on all the substantial changes in wood compositions occurring during the degradation process, confirming that the CrI is used to indicate the relative rather than the absolute amount of the crystalline cellulose in the whole wood material.

3.4. FTIR spectroscopy analysis

The IR spectra of sound and decayed Masson pine wood are shown in Fig. 3. FTIR spectra and the assignment of bands of wood samples have been extensively studied (Pandey & Pitman, 2003; Popescu et al., 2007, 2010). Owing to the complex nature of wood, most of the bands in the fingerprint region have contributions from all the wood constituents (Pandey & Pitman, 2003). To simplify the interpretation of IR bands and reflect exactly the chemical changes, the four characteristic absorption bands of holocellulose and two characteristic absorption ones of lignin are

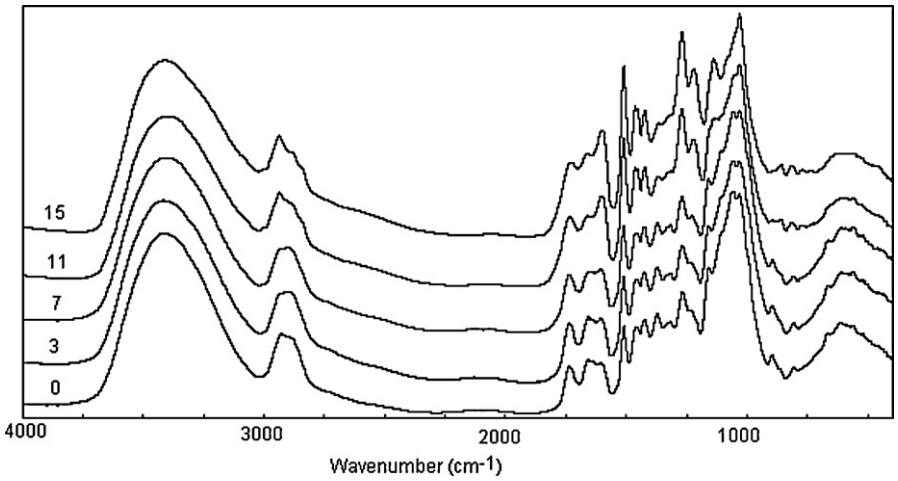

Fig. 3. FTIR spectra of Masson pine samples exposed to *W. cocos* for 0, 3, 7, 11 and 15 weeks.

Table 3
Relative intensities of typical bands for carbohydrates and lignin of Masson pine samples exposed to *W. cocos* for different durations.

Incubation time (week)	I_{1736}/I_{1510}	I_{1372}/I_{1510}	I_{1160}/I_{1510}	I_{897}/I_{1510}	I_{1510}/I_{1736}	I_{1225}/I_{1736}
0	0.567	0.377	0.506	0.208	1.763	0.207
3	0.617	0.331	0.425	0.172	1.620	0.154
7	0.508	0.288	0.405	0.143	1.967	0.260
11	0.302	0.114	–	0.029	3.312	0.787
15	0.194	0.071	–	–	5.163	1.377

used in this study as follows: 1736 cm^{-1} for unconjugated C=O stretch (hemicellulose), 1372 cm^{-1} for C–H deformation (cellulose and hemicellulose), 1160 cm^{-1} for C–O–C vibration (cellulose and hemicellulose), 897 cm^{-1} for C–H deformation (cellulose), 1510 cm^{-1} for aromatic skeletal vibration (lignin) and 1225 cm^{-1} for C–O stretch (lignin).

As shown in Fig. 3 and Table 3, the relative intensities of both carbohydrate bands and lignin bands showed only small change before 7 weeks, confirming the slow degradation during the initial stage of decay. The relative intensities of carbohydrate bands at 1736, 1372, 1160, and 897 cm^{-1} rapidly decreased with prolonging the incubation time from week 7 to week 15, with one at 1160 cm^{-1} almost absent at week 11 and one at 897 cm^{-1} absent at week 15. In contrast, the relative intensities of lignin bands at 1510 and 1225 cm^{-1} underwent a significant increase during the same incubation stage. This indicates that *W. cocos* preferentially decay carbohydrate fraction over lignin component. The change trends of IR absorption bands relative to carbohydrates and lignin confirmed the wet-laboratory analytical results.

It was especially mentioned that the relative intensity of hemicellulose peak at 1736 cm^{-1} did not have a rapid reduction until 11-week decay, and the decrease in the relative intensity was less for 1736 cm^{-1} when compared to the other three peaks resulting from carbohydrate, giving evidence that *W. cocos* has preferentially decayed the cellulose fraction over hemicellulose, and essential change of hemicellulose occurred during the late stage of degradation.

In FTIR the choice of reference spectral band is important if quantitative calculation is to be performed. In this study, the 1510 cm^{-1} band purely due to aromatic skeletal vibration of the benzene ring was used as a reference for lignin, while the 1736 and1372 cm^{-1} bands as carbohydrate references owing to the bands at 1160 and 897 cm^{-1} were absent during the later incubation stage. It was found that there was a good linear correlation between the ratios of band height of the lignin/holocellulose (I_{1510}/I_{1736} and I_{1510}/I_{1372}) and the Klason lignin content (R^2 = 0.96–0.99), which was similar to previous findings by Pandey and Pitman (2004). It was also interesting to find that a strong linear correlation existed between the ratios of band height of the lignin/holocellulose (I_{1510}/I_{1736} and I_{1510}/I_{1372}) and the holocellulose content, yielding R^2 values of 0.96. These results indicate that Klason lignin and holocellulose content for wood with a high level of decay can be measured by FTIR.

4. Conclusions

It was concluded that *W. cocos* preferentially degraded a carbohydrate portion over lignin component. Wood composition was first slowly degraded, then followed by a continued intensive destruction during the *W. cocos* degradation process. The slight degradation of amorphous cellulose and hemicellulose formed the entrance points for *W. cocos* to attack crystalline cellulose. Consequently, the whole cell wall was exposed to *W. cocos*, leading to the serious degradation of the cell wall.

Both alkali solubility and wood relative crystallinity were linearly related strongly to chemical composition of decayed wood. The change in holocellulose and Klason lignin content can be qualitatively and quantitatively analyzed by FTIR. The chemical component content, wood relative crystallinity, and FTIR spectra can provide complementary information on wood decay from different angles.

Acknowledgement

The financial support of National Key Technologies R&D Program for the 11th Five-Year Plan (project number: 2006BAD18B1002 and 2006BAD03A16) are gratefully acknowledged.

References

Adaskaveg, J. E., Blanchette, R. A., & Gilbertson, R. L. (1991). Decay of date palm wood by white-rot and brown-rot fungi. *Canadian Journal of Botany*, *69*, 615–629.

Andersson, S., Serimaa, R., Paakkari, T., Saranpää, P., & Pesonen, ·E. (2003). Crystallinity of wood and the size of cellulose crystallites in Norway spruce (*Picea abies*). *Journal of Wood Science*, *49*, 531–537.

Colom, X., Carrillo, F., Nogués, F., & Garriga, P. (2003). Structural analysis of photodegraded wood by means of FTIR spectroscopy. *Polymer Degradation and Stability*, *80*, 543–549.

Filley, T. R., Cody, G. D., Goodell, B., Jellison, J., Noser, C., & Ostrofsky, A. (2002). Lignin demethylation and polysaccharide decomposition in spruce sapwood degraded by brown rot fungi. *Organic Geochemistry*, *33*, 111–124.

Freire, C. S. R., Silvestre, A. J. D., Neto, C. P., Belgacem, M. N., & Gandini, A. J. (2006). Controlled heterogeneous modification of cellulose fibers with fatty acids: Effect of reaction conditions on the extent of esterification and fiber properties. *Journal of Applied Polymer Science*, *100*, 1093–1102.

Green, F., III, & Highley, T. L. (1997). Mechanism of brown-rot decay: Paradigm or paradox? *International Biodeterioration & Biodegradation*, *39*, 113–124.

Howell, C., Hastrup, A. C. S., Goodell, B., & Jellison, J. (2009). Temporal changes in wood crystalline cellulose during degradation by brown rot fungi. *International Biodeterioration & Biodegradation*, *63*, 414–419.

Irbe, I., Anderson, B., Chirkova, J., Kallavus, U., Andersone, I., & Faix, O. (2006). On the changes of pinewood (*Pinus sylvestris* L.) chemical composition and ultrastructure during the attack by brown-rot fungi *Postia placenta* and *Coniophora puteana*. *International Biodeterioration & Biodegradation*, *57*, 99–106.

Jin, L., Schultz, T. P., & Nicholas, D. D. (1990). Structural characterization of brown-rotted lignin. *Holzforschung*, *44*, 133–138.

Kubo, T., Terabayashi, S., Takeda, S., Sasaki, H., Aburada, M., & Miyamoto, K. I. (2006). Indoor cultivation and cultural characteristics of *Wolfiporia cocos* sclerotia using mushroom culture bottles. *Biological & Pharmaceutical Bulletin*, *29*, 1191–1196.

Lee, C. L. (1961). Crystallinity of wood cellulose fibers studies by X-ray methods. *Forest Products Journal*, *11*, 108–112.

Moigne, N. L., Jardeby, K., & Navard, P. (2010). Structural changes and alkaline solubility of wood cellulose fibers after enzymatic peeling treatment. *Carbohydrate Polymers*, *79*, 325–332.

Okino, E. Y. A., Santana, M. A. E., Resck, I. S., Alves, M. V., Falcomer, S., Cunha, V. A. S., et al. (2008). Liquid chromatography and solid state CP/MAS ^{13}C NMR techniques for chemical compound characterizations of cypress wood *Cupressus glauca* Lam. exposed to brown- and white-rot fungi. *Carbohydrate Polymers*, *73*, 164–172.

Pandey, K. K., & Pitman, A. J. (2003). FTIR studies of the changes in wood chemistry following decay by brown-rot and white-rot fungi. *International Biodeterioration & Biodegradation*, *52*, 151–160.

Pandey, K. K., & Pitman, A. J. (2004). Examination of the lignin content in a softwood and a hardwood decayed by a brown-rot fungus with the acetyl bromide method and Fourier transform infrared spectroscopy. *Journal of Polymer Science. Part A: Polymer Chemistry*, *42*, 2340–2346.

Pettersen, R. C. (1984). The chemical composition of wood. In R. Rowell (Ed.), *The chemistry of solid wood* (pp. 57–126). Washington D.C., US: American Chemical Society.

Popescu, C. M., Popescu, M. C., Singurel, G., Vasile, C., Argyropoulos, D. S., & Willfor, S. (2007). Spectral characterization of eucalyptus wood. *Applied Spectroscopy*, *61*, 1168–1177.

Popescu, C. M., Popescu, M. C., & Vasile, C. (2010). Structural changes in biodegraded lime wood. *Carbohydrate Polymers*, *79*, 362–372.

Segal, L., Creely, J. J., Martin, A. E., & Conrad, C. M. (1959). An empirical method for estimating the degree of crystallinity of native cellulose using the X-ray diffractometer. *Textile Research Journal*, *29*, 786–794.

Thygesen, A., Oddershede, J., Lilholt1, H., Thomsen, A. B., & Ståhl, K. (2005). On the determination of crystallinity and cellulose content in plant fibres. *Cellulose*, *12*, 563–576.

Wang, K.Q., Wang, L.Y., Wang, Y.B. (2006). Revulsive cultivation technique of *Wolfiporia cocos* sclerotia (in Chinese). State intellectual property office of the P.R.C., Pat. No. ZL 03128016.1.

Wellwood, R. W., Sastry, C. B. R., Micko, M. M., & Paszner, L. (1974). On some possible specific gravity holo- and -cellulose, tracheid weight/length and cellulose crystallinity relationships in a 500-year-old Douglas-fir tree. *Holzforschung*, *28*, 91–94.

Winandy, J. E., & Morrell, J. J. (1993). Relationship between incipient decay, strength, and chemical composition of Douglas-fir heartwood. *Wood and Fiber Science*, *25*, 278–288.